Available online at www.sciencedirect.com
SCIENCE DIRECT
Journal of Pharmaceutical and Biomedical Analysis 40 (2006) 271–280
JOURNAL OF PHARMACEUTICAL AND BIOMEDICAL ANALYSIS
www.elsevier.com/locate/jpba

Characterizing the conversion kinetics of carbamazepine polymorphs to the dihydrate in aqueous suspension using Raman spectroscopy

F. Tian [a], J.A. Zeitler [a], C.J. Strachan [a], D.J. Saville [a], K.C. Gordon [b], T. Rades [a,*]

[a] *School of Pharmacy, University of Otago, P.O. Box 913, Dunedin 9001, New Zealand*
[b] *Department of Chemistry, University of Otago, Dunedin, New Zealand*

Received 20 April 2005; received in revised form 18 July 2005; accepted 18 July 2005
Available online 16 September 2005

Abstract

In an aqueous environment, polymorphic forms I–III of carbamazepine all convert to the dihydrate. This study investigated the conversion of each polymorphic form individually and of a mixture of forms III and I to the dihydrate. Two batches of form I with different crystal morphology were used. Samples were dispersed independently in water at $23 \pm 1\,^{\circ}C$ and recovered at various timepoints varying from 10 to 210 min. Scanning electron microscopy, X-ray powder diffraction and Raman spectroscopy were used to characterize the initial polymorphic forms and the recovered samples after 210 min. Raman spectroscopy combined with partial least squares analysis was used to generate quantitative models of binary and ternary mixtures of the different polymorphic forms with the dihydrate. On the basis of these models the conversion kinetics of the polymorphic forms I–III were characterized. First-order kinetics with an unconverted portion were used to model the data ($R^2 \geq 0.95$). The unconverted portions ranged from 16 to 51% after dispersion for 210 min. The conversion kinetics were similar between polymorphic forms with comparable crystal morphology, but differed significantly between batches of the same polymorph (form I) with different crystal morphology. Furthermore, the conversion of forms III and I in the aqueous suspension was not influenced by the presence of the other polymorph when dispersed together.

Keywords: Carbamazepine; Polymorphism; Dihydrate; Kinetics; Morphology; Raman spectroscopy; Multivariate analysis

1. Introduction

Definitions and characteristics of polymorphism and pseudopolymorphism in the pharmaceutical field have been well described by several authors [1,2]. Polymorphism investigations are particularly important in drug and product development in the pharmaceutical industry since the properties of a formulated product such as bioavailability and stability are often directly related with the physicochemical properties of the existing polymorphs in the formulation.

Carbamazepine (CBZ) is an antiepileptic drug which has been in routine use for over 20 years [3]. Four polymorphs and a hydrate as well as other solvates of CBZ have been reported in the literature [4–6]. Among them, three principal polymorphs—forms I–III and the dihydrate (DH) have been well characterised [7–9]. CBZ form III is the form used in the marketed tablets and the most stable form at room temperature. However, a decreased bioavailability and other property changes such as hardening and disintegration of CBZ tablets after storage have been reported. These changes have been attributed to the formation of the DH [10–14]. Therefore, characterizing the conversion kinetics of CBZ form III to the DH is of great importance.

Efforts have been focused on investigating the transformation of CBZ form III to the DH for almost 20 years. Early in 1984, Laine et al. found that the conversion from form III to the DH was via a solution mediated mechanism where the growth of DH whiskers on the surface of form III could be observed clearly using light microscopy [15]. Quantification of the relative amounts of CBZ form III and DH in a mixture by XRPD was carried out by Suryanarayanan [16],

* Corresponding author. Tel.: + 64 3 479 5410; fax: +64 3 479 7034.
E-mail address: thomas.rades@stonebow.otago.ac.nz (T. Rades).

0731-7085/$ – see front matter © 2005 Elsevier B.V. All rights reserved.
doi:10.1016/j.jpba.2005.07.030

who subsequently reported a first-order kinetics of transformation from form III to the DH by quantifying the relative peak intensity changes of X-ray powder diffraction (XRPD) during the conversion [17]. Recently, Brittain [18] reported a novel way of characterizing the transformation kinetics of form III to the DH by detecting the fluorescence changes during the conversion since the polymorph and the DH show substantial fluorescence differences.

However, with the exception of fluorescence detection, techniques used for quantifying CBZ conversion to the DH thus far have only been XRPD, differential scanning calorimetry and Karl–Fischer titration, which are time consuming, and most importantly, polymorphic changes can potentially be induced during sample preparations such as filtration, grinding and drying.

Fourier transform (FT) Raman spectroscopy has attracted a high interest in the pharmaceutical field recently. Characterization of CBZ polymorphic forms and composition using FT-Raman spectroscopy were carried out by a number of authors [7,19–23], and quantitative analysis of the solid state polymorphic conversion from CBZ forms III to I has also been reported recently [24]. There are several advantages of using FT Raman spectroscopy as an analytical tool. Firstly, almost no sample preparation is required which facilitates quantitative analysis in polymorphic mixtures and formulations since polymorphic changes or spectral variances due to sample preparation are limited [25–28]. Secondly, slurry samples can be measured directly since water has a very weak Raman spectrum. This advantage of Raman spectroscopy has been successfully employed in the investigations of emulsion and suspension formulations [29–36]. Thirdly, the small sample size required combined with the non-invasive measurements all contribute to its great potential for application in pharmaceutical research and industry [37–40].

To facilitate quantitative analysis, multivariate analysis techniques such as principal component analysis (PCA) and partial least squares (PLS) have recently received considerable attention in quantitative spectroscopy. The combination of multivariate analysis with Raman spectroscopy has demonstrated a greatly increased ability in achieving precise quantification of various pharmaceutical systems [19,22,23,34,36,41–43].

In this study, FT-Raman spectroscopy is employed to investigate the conversion kinetics of three CBZ polymorphs—forms I–III separately, and also a mixture of forms I and III to the DH in aqueous suspension. PLS analysis is applied to the Raman spectra to obtain quantitative results.

2. Experimental

CBZ form III (Alphapharm Pty Ltd., Glebe, Australia) was used as received. CBZ form I was prepared by heating the source material at 150 °C for 3 h as described by Grzesiak et al. [4]. Two source materials were used for form I preparation: form I (first batch) from Sigma Chemical Company (St. Louis, MO) and form I (second batch) from Sigma–Aldrich Chemie (Munich, Germany). Form II was prepared by freeze-drying fresh DH. DH was prepared from the CBZ as received from Sigma Chemical Company (St. Louis, MO) by recrystallization from an ethanol–water mixture as reported by Krahn and Mielck [44]. All forms were confirmed by X-ray powder diffraction as reported previously [4,44].

The particle size of the different polymorphic forms was controlled by sieving them to the range 180–250 μm (Test sieves, Endecotts Ltd., England).

2.1. X-ray powder diffraction (XRPD)

XRPD analysis was used to confirm the nature of prepared CBZ polymorphs and also to characterize the recovered samples after dispersion in water for 210 min.

The XRPD measurements were performed using a Philips PW 1130/00 X-ray generator (Philips, Almelo, The Netherlands), and a Phililps PW 1050 goniometer (Philips, Almelo, The Netherlands). The X-ray generator was set to an acceleration voltage of 40 kV and a filament emission of 20 mA. The diffraction patterns were collected over the range of 8–40° (2θ) at a step size of 0.02° (2θ) using an aluminium sample holder. The diffractograms were displayed using Mac Diff version 4.0.5 software (A.J. Hall, Applied Geology, University of Strathclyde, England).

2.2. Scanning electron microscopy (SEM)

SEM micrographs were taken for the initial CBZ polymorphs and also the samples recovered after dispersion in water for 210 min. Samples were mounted onto a strip of double-sided carbon tape and sputter coated with a thin layer of gold–palladium under argon vacuum prior to analysis.

SEM (Cambridge Instrument, Stereoscan 360) was performed using a 15 kV beam acceleration voltage. Micrographs were recorded using a PGTE Mitsubishi video/copy processor.

2.3. Raman spectroscopy

The FT-Raman instrument consisted of a Bruker FRA 106/S FT-Raman accessory (Bruker Optik, Ettlingen, Germany) with a Coherent Compass 1064-500N laser (Coherent Inc, Santa Clara, USA) attached to a Bruker IFS 55 FT-IR interferometer, and a D 425 Ge diode detector. Analysis was carried out at room temperature utilizing a laser wavelength of 1064 nm (Nd:YAG laser) and a laser power of 105 mW. Back-scattered radiation was collected at an angle of 180°. Samples were packed into an aluminum cup and a total of 16 scans was averaged for each sample at a resolution of 4 cm^{-1}. Sulfur was used as reference

standard to monitor the wavenumber accuracy. OPUS^{TM} 5.0 (Bruker Optik, Ettlingen, Germany) was used for all spectral analysis.

2.4. Mixture quantitation

2.4.1. Binary model prepared from recovered slurries

Binary mixtures of CBZ form I (first batch) and DH, and form II and DH were prepared separately in triplicate at 20% (w/w) intervals from 0 to 100% form I (form II) in DH (20 mg per sample). Each powder mixture was transferred into a 2 ml glass tube and a small magnetic stirrer was added. Immediately after adding 1 ml distilled water, the tube was capped, shaken up and down once and put into a water jacketed beaker. Each sample was stirred for 10 s, and then recovered by pouring the dispersion onto two layers of filtration paper to remove excess water. The CBZ slurry was then transferred into three sample cups consecutively (about 1 mg sample per cup). The Raman spectra were recorded immediately after filling the sample cups.

As CBZ is only very slightly soluble in water at room temperature [45] it was assumed that the dissolution of CBZ had no influence on its solid dispersion concentration. Also, in order to confirm that there was no change in the DH during dispersion, pure DH was dispersed in water for 210 min and then recovered for analysis as described above.

2.4.2. Binary models prepared from dry powder

Using geometric mixing, CBZ polymorphs of forms I (first batch), II and III were blended separately with DH to form binary physical mixtures at 20% (w/w) intervals from 0 to 100% CBZ anhydrate in DH (20 mg per sample). Each concentration was prepared in triplicate and measured by Raman spectroscopy.

2.4.3. Ternary model prepared from dry powder

Thirty-three ternary mixtures (100 mg per mixture) of form I (second batch), form III and DH were prepared as an independent sample set for the ternary model, with randomly varying concentrations of each component.

2.4.4. Multivariate analysis

Multivariate analysis was performed using the Quant2 package that accompanies OPUS^{TM} software (Bruker Optics, Germany). The selection of spectral regions for calibration was based on the wavenumber regions that showed the largest differences between the components and therefore provided the greatest contribution to the linear regression equation for the analyte. All spectra were mean centered. Although every effort was made to pack the sample cups consistently, multiplicative scattering correction (MSC) was applied to correct spectra intensity differences due to packing differences. Other spectral preprocessing consisted of first derivative calculation if necessary to remove baseline differences. The calibration models were calculated using the PLS algorithm and cross-validation (one sample removed per cycle). The root-mean-squared errors of cross validation (RMSECV) were determined for each number of factors.

2.5. Kinetics studies

Each pure polymorph—forms I (first and second batch), II and III was weighed (40 mg per sample) into a 2 ml glass tube. For the mixture of forms I (second batch) and III, 20 mg of each form was poured together into a 2 ml glass tube (40 mg per mixture). All samples were prepared in triplicate. After adding a small magnetic stirrer into each tube, water (2 ml) was added and then the stoppered tube was placed into 100 ml water jacketed beakers. The dispersion temperature was controlled at $23 \pm 1\,^{\circ}C$. Independent samples were dispersed for each of the time intervals of 10, 30, 60, 90, 120, 180 and 210 min, and recovered for measurement.

The differences of the conversion kinetics between polymorphic forms were tested by one-way analysis of variance (ANOVA) and Tukey's pairwise comparisons (significance level was 0.05) using Minitab 12.1 software (Minitab Ltd., USA).

3. Results and discussion

3.1. Characterization of the initial CBZ polymorphs

3.1.1. XRPD

The X-ray diffractograms of each CBZ polymorph (Fig. 1) agreed well with those reported in the literature [4,44]. However, the relative height of some peaks was different between the two batches of form I, which may be caused by different crystal habits. As shown by SEM (Fig. 2), form I (first

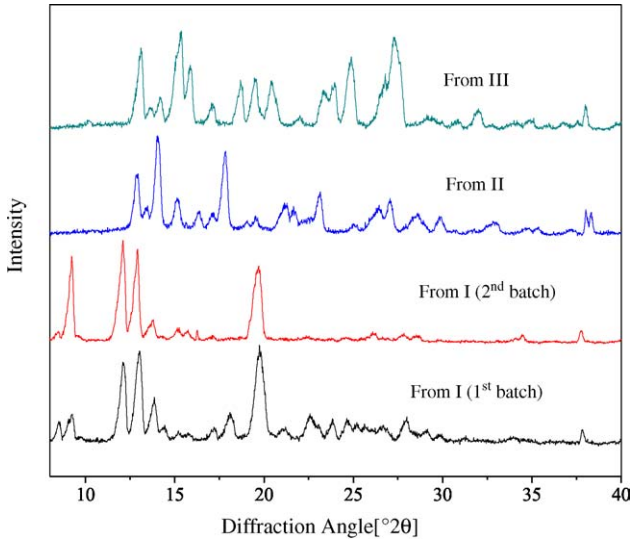

Fig. 1. X-ray diffractograms of the initial CBZ polymorphs.

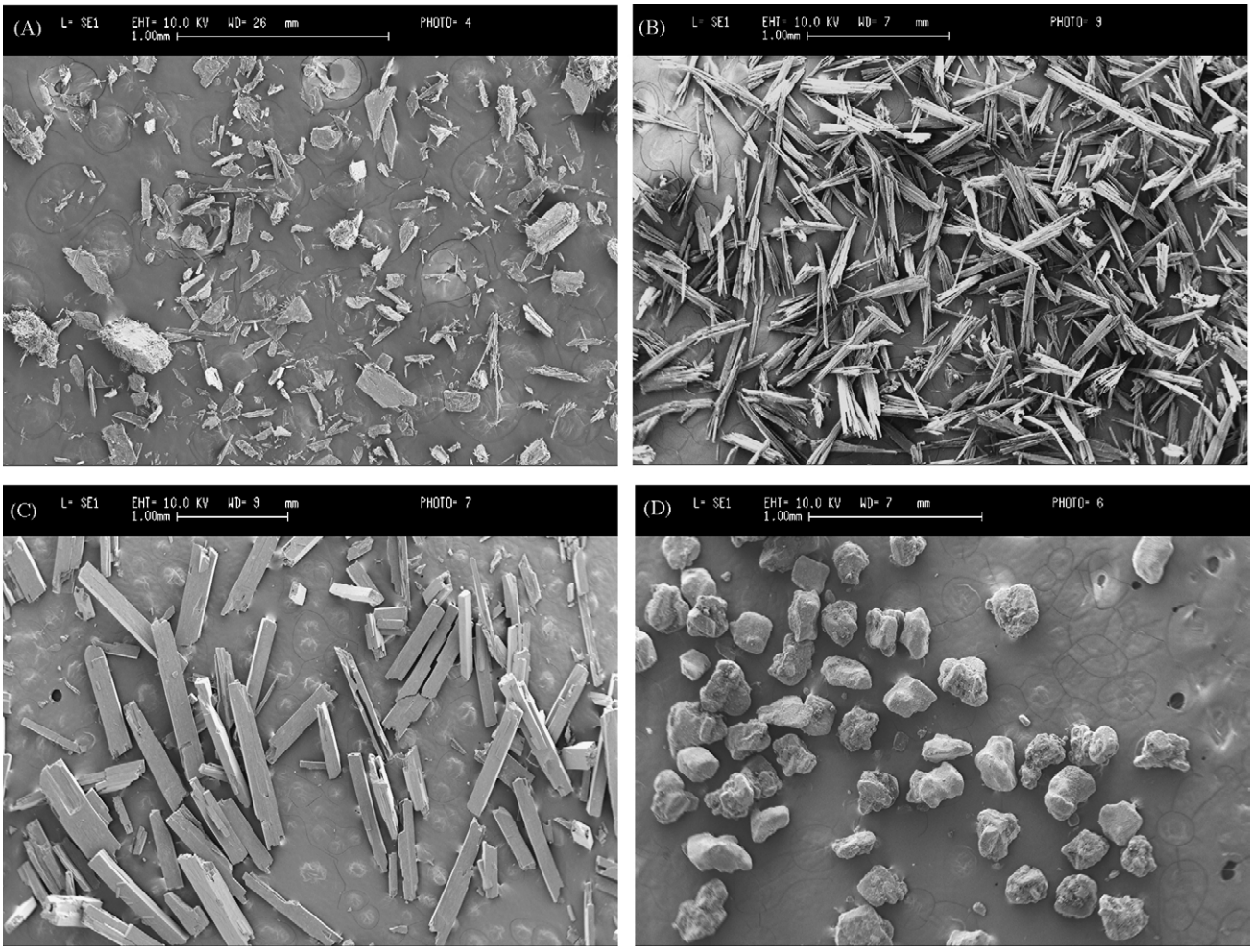

Fig. 2. SEM micrographs of CBZ polymorphs: (A) form I (first batch); (B) form I (second batch); (C) form II; (D) form III (horizontal scale bars: 1.00 mm).

batch) consisted of needle-like crystals, therefore, preferred orientation was likely to be induced when it was packed in the XRPD sample holder.

3.1.2. SEM

The morphology of all CBZ polymorphs—form I (first and second batch), II and III which were used for the kinetics studies is shown in Fig. 2.

As mentioned above, the characteristic peak positions in the X-ray diffractograms of the two batches of form I agreed well with each other although some relative peak heights differed. However, their morphology was obviously different. Form I (first batch) consisted mainly of prism-like particles (Fig. 2A), while form I (second batch) consisted of needle-like aggregates (Fig. 2B). Form II also exhibited a needle-like morphology but the needles appeared more densely packed than the form I needles (Fig. 2C). Form III showed a typical prism-like shape (Fig. 2D) [6].

3.1.3. Raman spectroscopy

Raman spectra for the initial CBZ polymorphic forms are shown in Fig. 3. There were many spectral differences between these polymorphs (indicated by the arrows). Since crystal shape has much less influence on the Raman spectrum than on the X-ray diffractogram [46], Raman spectra for the two batches of form I were identical.

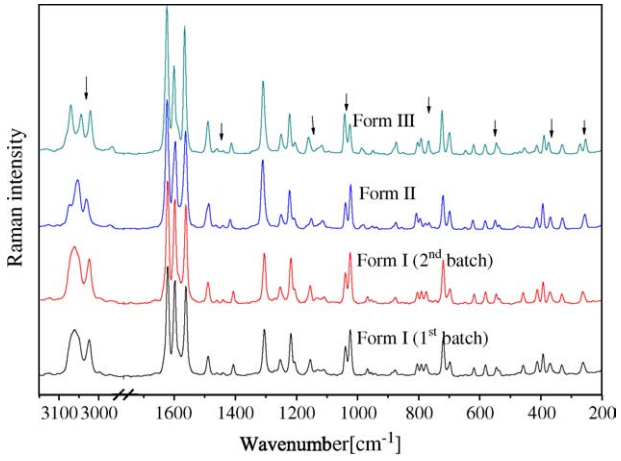

Fig. 3. Raman spectra of the initial CBZ polymorphs. (Arrows show area of spectral differences between the samples.)

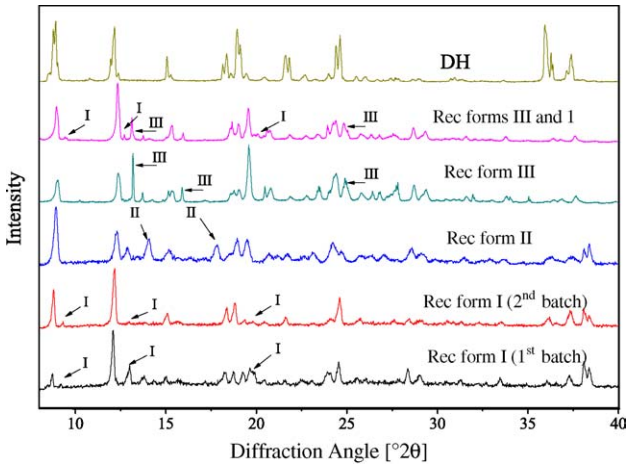

Fig. 4. X-ray diffractograms of the recovered (rec) forms and the dihydrate (DH). (Arrows show characteristic peaks of forms I–III.)

3.2. Characterization of the samples recovered after 210 min dispersion in aqueous suspension

3.2.1. XRPD

The diffractograms for the recovered samples from the 210 min dispersions are shown in Fig. 4. The DH has characteristic peaks at 8.9°, 12.1° and 18.7° (2θ) which could be found in the diffractograms of all the recovered samples. Also, characteristic peaks for each polymorph remaining in the recovered samples could be seen (indicated by the arrows in Fig. 4). The diffractogram of the recovered form I (second batch) was very similar to that of the DH which indicated a high degree of conversion.

3.2.2. SEM

The morphology of the recovered samples from the 210 min dispersions is shown in Fig. 5. A distinct and common feature seen in Fig. 5A, C and D was some areas of closely packed, smooth surfaces. However, this feature was absent in Fig. 5B, where almost all crystals were of needle-like shape (typical DH morphology) [15,21,47]. This confirmed the finding from XRPD that form I (second batch) converted mostly to the DH after 210 min dispersion, while the other polymorphs – forms I (first batch), II and III – still had a certain amount of original crystals remaining in the suspension.

3.2.3. Raman spectroscopy

Raman spectra for all the recovered samples showed different peak patterns to their initial polymorphs and also an increased similarity to that of the DH, especially for the recovered form I (second batch). Although Raman spectra for the two batches of form I were exactly the same (Fig. 3), differences can be seen in the spectra (around 3050, 1000, 800 and 400 cm^{-1}) of the recovered samples due to different extents of conversion. The spectrum of the slurry recovered from the pure DH dispersion is also shown in Fig. 6, and is identical to the DH spectrum.

3.3. Quantitative studies

3.3.1. Quantitation of the binary mixtures

Table 1 shows the parameters used for the quantitative models of all binary mixtures. For all models, the RMSECV was less than 8% suggesting a good predictive ability of the models. The lower RMSECV for the slurry model is probably due to better mixing. However, as described in the next section, slurry models are prone to polymorphic conversion due to the presence of the water in their preparation, which can affect the model accuracy.

Furthermore, as particle size has been reported to influence peak intensity and/or width [35,48,49], form III of different size ranges was measured by Raman spectroscopy. The spectral variances became negligible after processing (MSC and first derivative calculation) for PLS analysis. Furthermore, the ability of applying PLS to correct particle size effects on the relative peak intensities in Raman spectra for quantitative analysis of polymorphic forms has been reported by Zhou et al. [50].

3.3.2. Conversion kinetics of the pure CBZ polymorphic forms

As shown above, two methods were used for the model preparation of form I—recovered slurries and dry powder. Therefore, conversion kinetics based on the two types of binary models were plotted together for form I (Fig. 7) in order to compare differences between these two models. An assumption was made that each polymorphic form converted directly to the DH and not via some other form.

For each batch of form I, the slurry and powder models agreed very well with each other, confirming the applicability of both models when using them for kinetics studies. However, for the model using the recovered slurries to be accurate, it is necessary that no polymorph converts to the DH during the dispersion of the polymorph in water, which may not be the case for very fast converting samples, such as form II. Although the conversion trends of form II predicted by the two models were similar, the actual values of the DH formation predicted from the slurry model were about 20% less than those for the powder model (Fig. 8). This difference was due to conversion to the DH in the 10 s dispersion preparation. Since calibration models using dry powder mixtures to quantify polymorphic conversion in aqueous suspension were found to be accurate by Ono et al. [32] using both off-line and in situ measurements, quantitative models using dry powder mixtures were prepared for the subsequent studies.

As first-order kinetics have been reported for the conversion of CBZ form III to the DH in aqueous solution by a few authors [17,18], the same kinetics were evaluated for the conversion of all CBZ forms. Fig. 9 shows conversion profiles for all these forms using their corresponding binary quantitative models, and first-order kinetics models with an unconverted portion were fitted.

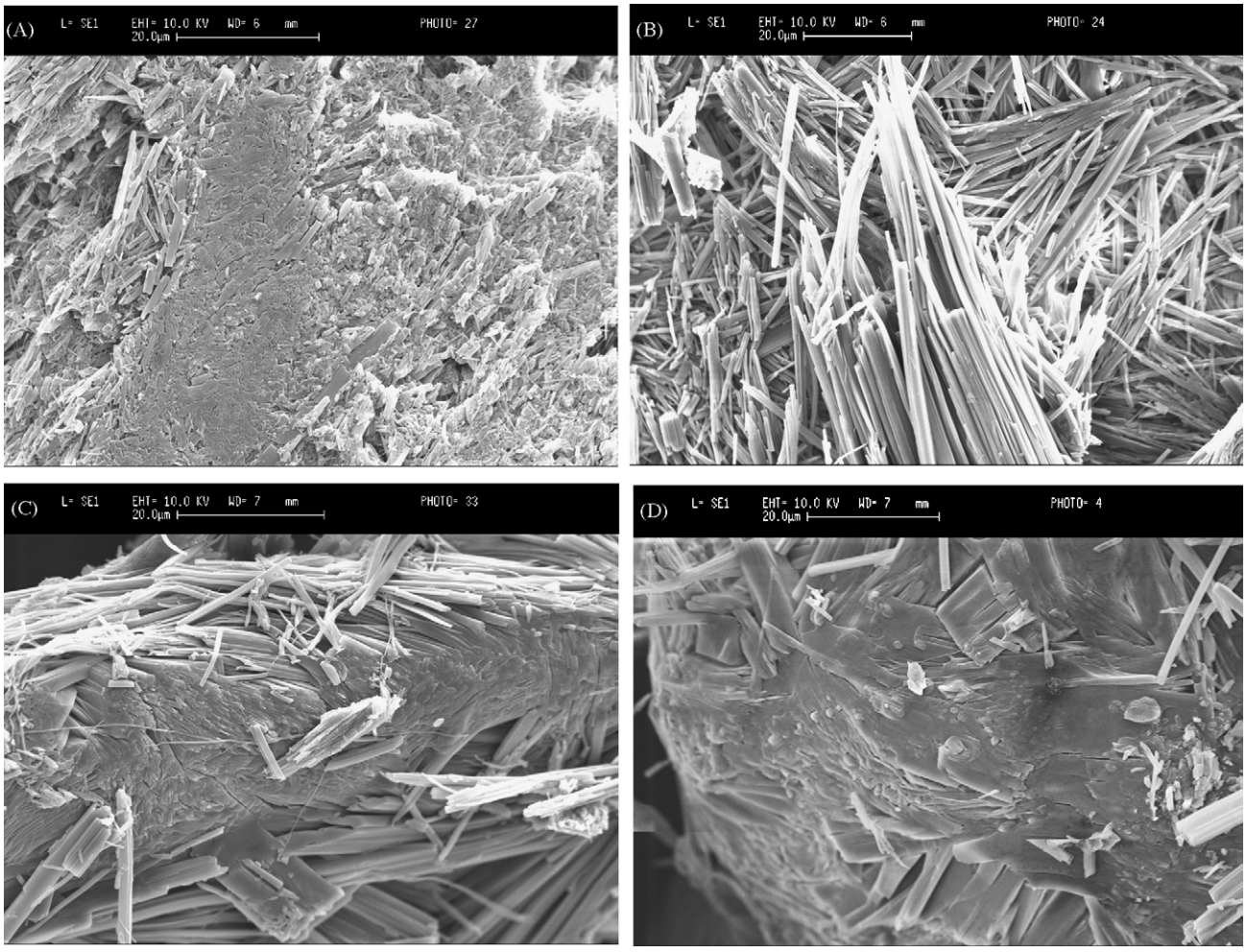

Fig. 5. SEM micrographs of the recovered forms: (A) form I (first batch); (B) form I (second batch); (C) form II; (D) form III (horizontal scale bars: 20.0 μm).

Table 2 shows the calculated rate constants (k) and the unconverted portions (B) after 210 min dispersion in aqueous suspension (t = time):

$$y = B + A\,e^{-kt} \quad (1)$$

As shown above, there was an unconverted portion after 210 min dispersion fitted for all CBZ forms, which indicated conversion to the DH was not complete. This incomplete conversion was also supported by the results from SEM, XRPD, and might be caused by the DH needles forming at the surface

Table 1
Parameters used in the generation of the binary models and model assessment

	Recovered slurries		Dry powder		
	Form I (first batch)/DH[a]	Form II/DH[a]	Form I (first batch)/DH[a]	Form II/DH[a]	Form III/DH[a]
Spectral regions (cm^{-1})	1514.3–1473.8	3099.7–3003.3	1514.3–1473.8	3236.7–2849.0	1685.9–1473.8
	1282.8–1234.6	1722.6–1390.8	1282.8–1234.6	1682.1–1469.9	1269.3–1099.6
	1147.8–1082.2	1277.0–1080.3	1147.8–1082.2	1433.3–1388.9	740.8–706.1
	1061.0–1008.2	906.7–733.1	1061.0–1008.2	1273.2–1234.6	640.5–557.6
	818.0–760.1	661.7–603.9	818.0–760.1	1176.7–1093.8	405.2–349.3
	630.9–609.5	351.2–308.8	630.9–609.5	899.0–862.3	
	596.2–528.6		596.2–528.6	740.8–519.0	
	596.2–528.6		596.2–528.6	499.7–430.3	
				347.3–308.8	
Factors used	3	2	2	2	2
RMSECV (%)	1.70	3.12	4.56	5.39	7.71
R^2	0.998	0.991	0.982	0.975	0.952

[a] Mixture.

Table 2
First-order rate constants and unconverted portions after 210 min dispersion in aqueous suspension for each CBZ form

	Crystal habit			
	Prism-like crystals		Needle-like crystals	
	Form I (first)	Form III	Form I (second)	Form II
Rate constant (min^{-1})	0.0196 ± 0.0037	0.0529 ± 0.0134	0.0982 ± 0.0182	0.174 ± 0.021
Unconverted portion (%)	34.6 ± 3.8	51.1 ± 1.4	16.5 ± 1.9	27.9 ± 0.4

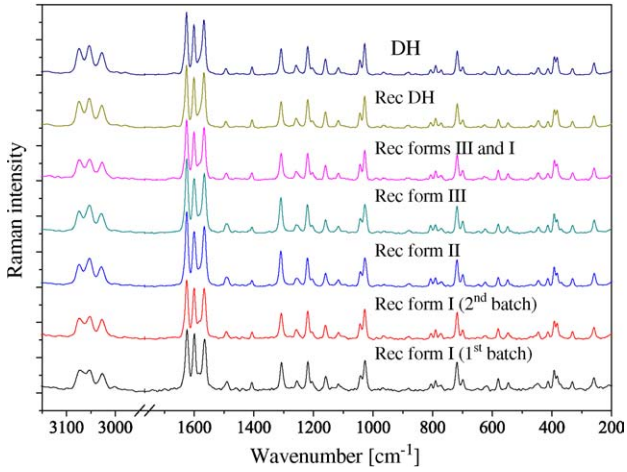

Fig. 6. Raman spectra of DH and the recovered (rec) CBZ samples.

of the particles and then covering the surface of the remaining anhydrate, thus slowing down or even stopping further conversion.

Other possible kinetic models based on solid-state reaction mechanisms were also considered [51–53] (Table 3).

The best fitting and simplest model was a first-order kinetics model (M1) with an unconverted portion ($R^2 \geq 0.949$).

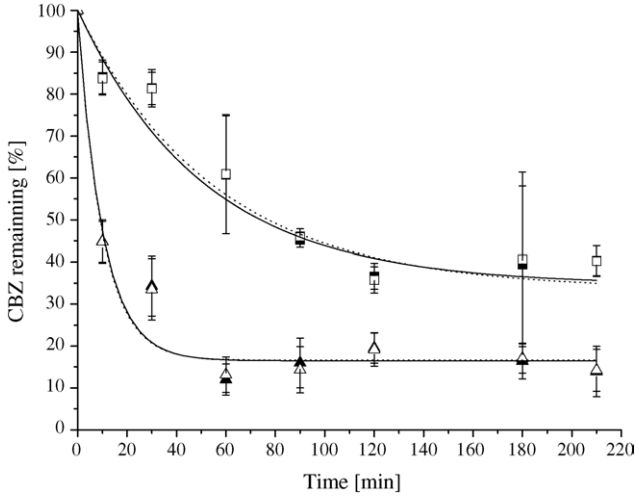

Fig. 7. Conversion of form I based on the two types of binary calibration models: form I (first batch) based on model from (■) dry powder and (□) recovered slurries; form I (second batch) based on model from (▲) dry powder and (△) recovered slurries. Values based on the model from dry powder are interpolated by the solid lines; values based on the model from recovered slurries are interpolated by the dotted lines.

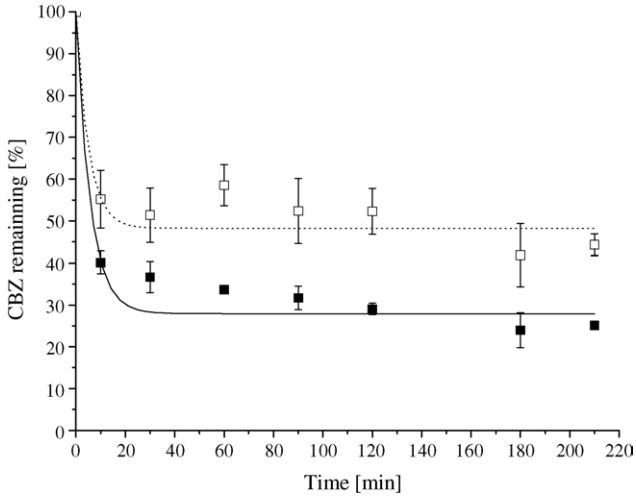

Fig. 8. Conversion of form II based on the two types of binary calibration models: from (■) dry powder and (□) recovered slurries. Values based on the model from dry powder are interpolated by the solid lines; values based on the model from recovered slurries are interpolated by the dotted lines.

However, the form II kinetics appeared to be best described by a two phase model (M2) consisting of a very fast initial conversion followed by a sustained slow conversion ($R^2 = 0.999$). This fast initial conversion may be related to voids in the form II crystal structure, which greatly facilitated the penetration of water into its crystals [6].

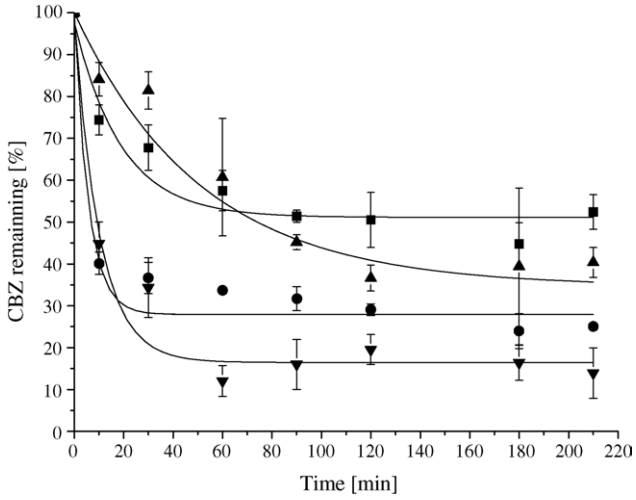

Fig. 9. Conversion of CBZ polymorphs as predicted by the binary models: (▲) form I (first batch); (■) form III; (●) form II; (▼) form I (second batch).

Table 3
Equations for common kinetic models

	Equation	Mechanism
M1	$y = B + A\,e^{-kt}$	First-order mechanism with an unconverted portion
M2	$y = B + A_1\,e^{-(t-t_0)k_1} + A_2\,e^{-(t-t_0)k_2}$	Exponential two phase decay
M3	$y/y_0 = e^{-(kt)^2}$	Two-dimensional growth of nuclei mechanism (Avrami equation) [51–53]
M4	$y/y_0 = e^{-(kt)^3}$	Three-dimensional growth of nuclei mechanism (Avrami equation) [51,53]
M 5	$M^{1/3} = M_0^{1/3} - kt$	Dissolution of monodispersed powder under sink conditions (Hixon–Crowell equation) [54]

Further samples would have been desirable in the early phase for the rapidly converting forms. However, this was limited due to the off-line nature of the measurement where high variances were likely to be induced by sampling errors in the fast converting phase.

One-way ANOVA was used to test if there were significant differences in the conversion kinetics between the crystals of similar shape but different polymorphic form. There was no significant difference between form I (first batch) and form III prisms.

Also, for form I (second batch) and form II needles, no significant differences were detected at every conversion time point except 60 and 90 min. The similar conversion rates may be due to forms II and I needles having very similar hydrogen bonding in their crystal structures [4]. Also, form I (second batch) consisted of aggregated needles (Fig. 2), which might be deaggregated, thus increasing the exposed surface area which explains its highest conversion extent among all the forms (almost 90% conversion at 210 min).

However, the conversion profiles of the two batches of form I with different crystal morphology were significantly different. The needle-like form I (second batch) had a higher conversion rate (about five times faster) and conversion extent (about 30% more converted to the DH after 210 min dispersion).

It can be concluded that for samples of the same sieve-size fraction, crystal morphology has a greater effect than the polymorphic form on the conversion kinetics of CBZ to the DH in aqueous suspension. Since the conversion of CBZ anhydrates to the DH are solution mediated [47], surface area may be a critical parameter to explain the different conversion profiles between these CBZ forms. The actual surface area for these samples was not determined due to the limited amounts of samples available in this study, however, from SEM micrographs, the surface area could be estimated to be ranked as D < A/C < B (Fig. 2).

The first-order rate constant calculated for form III conversion agreed well with that reported by Yong and Suryanarayanan [17], confirming the applicability of this method for the kinetics studies. However, there was a difference in the extent of conversion where form III reached a plateau of 49% conversion to the DH in this experiment but converted completely within 60 min in the study reported in the literature. This may be explained by the available surface area for the continuing nucleation being limited by the attachment of the DH crystals to the unchanged anhydrate. Mechanical agitation may facilitate the removal of these crystals and thus allow further conversion. The stirring system used in this study was of much lower force than that used by Yong and Suryanarayanan and it was observed under SEM that DH needles were attached to or covered the surface of the CBZ samples recovered after 210 min dispersion. However, as the particle size range and the morphology of the samples used by Yong and Suryanarayanan were not specified in their paper, the different extents of conversion might also be due to particle morphology and size differences between the initial samples.

3.3.3. Quantitation of the ternary mixtures

The quantitative ternary model was generated with a RMSECV of 3% or less for all components which suggested a very good predictive ability of the model.

3.3.4. Conversion kinetics of the mixture of forms I (second batch) and III (50:50)

The kinetics values of forms I and III from the ternary model were plotted together with the halved values based on the binary models (Fig. 10), since the sample concentration of forms I and III in the mixture was half that in their separate dispersions. Eq. (1) was fitted for forms I and III respectively and their first-order rate constants and the unconverted portions based on the binary and ternary models are listed in Table 4.

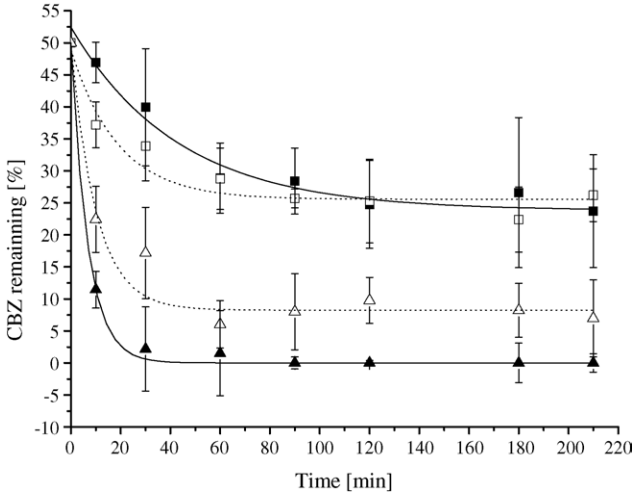

Fig. 10. Conversion of forms III and I predicted by binary and ternary models: form III based on (■) ternary and (□) binary models; form I based on (▲) ternary and (△) binary models. Values from the ternary models are shown as solid lines; values from the binary models are shown as dotted lines.

Table 4
First-order rate constant and unconverted portion for forms III and I (second batch) based on both binary and ternary models

CBZ forms	First-order rate constant (min^{-1})		Unconverted portion (%)	
	Binary models	Ternary model	Binary models	Ternary model
Form I (second batch)	0.098 ± 0.018	0.147 ± 0.025	34.6 ± 3.8	0.010 ± 0.300
Form III	0.053 ± 0.013	0.023 ± 0.018	51.1 ± 1.4	23.8 ± 6.4

One-way ANOVA showed that there was no significant difference between the conversion rates for form III alone (using the binary model) and form III in the mixture (using the ternary model) except for the values at 10 min, although the rate constants and the unconverted portion were slightly differently predicted by two models (Table 4).

For form I, there were significant differences between values at every time point except 60 min. Although this difference needs to be investigated further, it may be due to the small amount of form I remaining in the dispersion and the small proportion of the recovered sample measured (of each 40 mg dispersed sample, three samples each of about 1 mg were measured after recovery). Furthermore, as shown by XRPD (Fig. 4), some characteristic peaks of form I can still be seen in the recovered samples from the mixture of forms III and I after dispersing for 210 min, albeit small.

It may be concluded that there was no interaction or influence on form III conversion when dispersed together with form I as the conversion kinetics of form III were almost the same as for the pure form III dispersion. The conversion kinetics of form I in the mixture were not clearly detected. In a future study, a Raman probe will be used to investigate these polymorphic systems, where the sampling errors will be minimized and the feasibility of online accurate quantitative analysis of these polymorphic forms and conversion processes in suspension will be investigated.

4. Conclusion

The current study has shown that Raman spectroscopy and multivariate analysis can in principle be used to characterize and quantify conversions of CBZ polymorphs to the DH in aqueous suspension.

The crystal morphology rather than the polymorphic form of CBZ was found to affect its conversion kinetics, indicating the importance of surface properties of crystals for solution mediated conversion. Investigations to obtain a deeper understanding of the crystal surface and morphology changes for CBZ when dispersed in aqueous suspension will be carried out in further studies using Raman microscopy.

References

[1] S.R. Vippagunta, H.G. Brittain, D.J.W. Grant, Adv. Drug Delivery Rev. 48 (2001) 3–26.
[2] J. Bernstein, Polymorphism in Molecular Crystals, Oxford University Press, UK, 2002, pp. 1–28.
[3] R. Hartley, J. Aleksandrowicz, P.C. Ng, B. McLain, C.J. Bowmer, W.I. Forsythe, Br. J. Clin. Prac. 44 (1990) 270–273.
[4] A.L. Grzesiak, M.D. Lang, K. Kim, A.J. Matzger, J. Pharm. Sci. 92 (2003) 2260–2271.
[5] M.D. Lang, J.W. Kampf, A.J. Matzger, J. Pharm. Sci. 91 (2002) 1186–1190.
[6] M.M.J. Lowes, M.R. Caira, A.P. Lotter, J.G. Van Der Watt, J. Pharm. Sci. 76 (1987) 744–752.
[7] L.E. McMahon, P. Timmins, A.C. Williams, P. York, J. Pharm. Sci. 85 (1996) 1064–1069.
[8] J. Dugué, J. Ceolin, J.C. Rouland, F. Lepage, Pharm. Acta Helv. 66 (1991) 307–310.
[9] R. Ceolin, S. Toscani, M.F. Gardette, V.N. Agafonov, A.V. Dzyabchenko, B. Bachet, J. Pharm. Sci. 86 (1997) 1062–1065.
[10] W.L. Bell, I.L. Crawford, G.K. Shiu, Epilepsia 34 (1992) 1102–1104.
[11] M.C. Meyer, A.B. Straughn, J.J. Eric, G.C. Wood, F.R. Pelsor, V.P. Shah, Pharm. Res. 9 (1992) 1612–1616.
[12] Anon., Am. J. Hosp. Pharm. 47 (1990) 958.
[13] M.M. Lowes, Am. J. Hosp. Pharm. 48 (1991) 2130–2131.
[14] H. Al-Zein, L.E. Riad, A. Abd-Elbary, Drug Dev. Ind. Pharm. 25 (1999) 223–227.
[15] E. Laine, V. Tuominen, P. Ilvessalo, P. Kahela, Int. J. Pharm. 20 (1984) 307–314.
[16] R. Suryanarayanan, Pharm. Res. 6 (1989) 1017–1024.
[17] W.W.L. Yong, R. Suryanarayanan, J. Pharm. Sci. 80 (1991) 496–500.
[18] H.G. Brittain, J. Pharm. Sci. 93 (2003) 375–383.
[19] M.E. Auer, U.J. Griesser, J. Sawatzki, J. Mol. Struct. 661–662 (2003) 307–317.
[20] L.S. Taylor, F.W. Langkilde, J. Pharm. Sci. 89 (2000) 1342–1353.
[21] P.A. Anquetil, C.J.H. Brenan, C. Marcolli, I.W. Hunter, J. Pharm. Sci. 92 (2003) 149–160.
[22] D. Pratiwi, J.P. Fawcett, K.C. Gordon, T. Rades, Eur. J. Pharm. Biopharm. 54 (2002) 337–341.
[23] C.J. Strachan, D. Pratiwi, K.C. Gordon, T. Rades, J. Raman. Spectrosc. 35 (2004) 347–352.
[24] L.E. O'Brien, P. Timmins, A.C. William, P. York, J. Pharm. Biomed. Anal. 36 (2004) 335–340.
[25] L.S. Taylor, G. Zografi, Pharm. Res. 15 (1998) 755–761.
[26] S.N. Campbell Roberts, A.C. Williams, I.M. Grimsey, S.W. Booth, J. Pharm. Biomed. Anal. 28 (2002) 1135–1147.
[27] D.P. Schweinsberg, Y.D. West, Spectrochim. Acta Part A: Mol. Biomol. Spectrosc. 53A (1997) 25–34.
[28] F.W. Langkilde, J. Sjoblom, L. Tekenbergs-Hjelte, J. Mrak, J. Pharm. Biomed. Anal. 15 (1997) 687–696.
[29] K. Ito, T. Kato, T. Ona, J. Raman Spectrosc. 33 (2002) 466–470.
[30] T. De Beera, G. Vergoteb, W. Baeyensa, Eur. J. Pharm. Sci. 23 (2004) 355–362.
[31] H. Wiskstrom, P.J. Marsac, L.S. Taylor, J. Pharm. Sci. 94 (2004) 209–219.
[32] T. Ono, J.H. ter Horst, P.J. Jansens, Cryst. Growth Des. 4 (2004) 465–469.
[33] F. Wang, J.A. Wachter, F.J. Antosz, K.A. Berglund, Org. Proc. Res. Dev. 4 (2000) 391–395.
[34] C. Starbuck, A. Spartalis, L. Wai, J. Wang, P. Fernandez, C.M. Lindemann, G.X. Zhou, G. Zhihong, Cryst. Growth Des. 2 (2002) 515–522.
[35] B.O. Sullivan, P. Barrett, G. Hsiao, A. Carr, B. Glennon, Org. Proc. Res. Dev. 7 (2003) 977–982.

[36] A. Jorgensen, J. Rantanen, M. Karjalainen, L. Khriachtechev, E. Rasanen, Y. Jliruusi, Pharm. Res. 19 (2002) 1285–1291.
[37] T. Vankeirsbilck, A. Vercauteren, W. Baeyens, G. Van der Weken, F. Verpoort, G. Vergote, J.P. Remon, Trends Anal. Chem. 21 (2002) 869–877.
[38] G. Fini, J. Raman Spectrosc. 35 (2004) 335–337.
[39] A.C. Williams, in: I.R. Lewis, H.G.M. Edwards (Eds.), Handbook of Raman Spectroscopy, Marcel Dekker Inc., New York, 2001, pp. 575–615.
[40] W.P. Findlay, D.E. Bugay, J. Pharm. Biomed. Anal. 16 (1998) 921–930.
[41] M-S. Ku, H. Chung, Bull. Korean Chem. Soc. 20 (1999) 159–162.
[42] A.G. Ryder, G.M. O'Connor, T.J. Glynn, J. Raman Spectrosc. 31 (1999) 221–227.
[43] P.S. Jacobsson, M. Carlsson, U. Jonsson, G. Nilsson, J. Pharm. Biomed. Anal. 13 (1995) 415–417.
[44] F.U. Krahn, J.B. Mielck, Pharm. Acta Helv. 62 (1987) 247–254.
[45] M. Windholz, The Merck Index, 10th ed., Merck & Co. Inc, Rahway, NJ, 1983, p. 246.
[46] A. Forster, C.K. Gordon, D. Schmierer, N. Soper, V. Wu, T. Rades, Int. J. Vib. Spectrosc. 2 (2) (1998) 12.
[47] D. Murphy, F. Rodríguez-Cintrón, B. Langevin, R.C. Kelly, N. Rodriguez-Hornedo, Int. J. Pharm. 246 (2002) 121–134.
[48] E.M.I. Salje, U. Tech, F.R.G. Hanover, J. Appl. Crystallogr. 6 (1973) 442–446.
[49] H. Wang, C.K. Mann, T.J. Vickers, Appl. Spectrosc. 56 (2002) 1538–1544.
[50] G. Zhou, J. Wang, Zhihong Ge, Yongkui Sun, Am. Pharm. Rev. 5 (2002) 74–80.
[51] M. Otsuka, M. Ishii, Y. Matsuda, Colloids Surf. B 23 (2002) 73–82.
[52] K. Ikegami, Y. Kawashima, H. Takeuchi, H. Yamamoto, N. Isshiki, D. Momose, K. Ouchi, Pharm. Res. 19 (2002) 1439–1445.
[53] M. Otsuka, M. Ishii, Y. Matsuda, AAPS PharmSciTech 4 (2003) E5 (electronic resource), Article 19 (http://www.pharmscitech.org).
[54] A. Martin, Physical Pharmacy, 4th ed., Lea & Feiger, Philadelphia, 1993, pp. 333–334.